Design, prototyping and mechanical testing of a trifilar deployable helix antenna for CubeSat applications

M. Longato(1) *, M. Honeth(1), G. S. Aglietti(1) L. Marcaccioli(2) M. Capoduri(2)

(1) Space Institute - Te Pūnaha Ātea (TPA-SI), University of Auckland, Auckland,1010, New Zealand
2) RF Microtech Srl, Perugia, Italy

*Corresponding author, mattia.longato@auckland.ac.nz

ABSTRACT

Deployable helical antennas are often used in space in the VHF and UHF transmission bands because they provide high gain, large bandwidth, and high directivity with circular polarization while maintaining relatively low fabrication complexity. Usually, these deployable antennas are composed of a main foldable, non-conducting isolated structure which acts as the helicoid support for the main conducting wire element. Generally, these antennas need to be kept stowed during launch and deployed once in space. This paper presents an innovative resettable trifilar helicoid deployable antenna where three independent helix-shaped metal wires are employed to perform both functions: the deployable support structure and the main conductor as a single entity. The initial design and manufacturing process of the helix-shaped metal wires are illustrated in this work together with the respective numerical simulations to ensure the correct electrical performance and the desired deployed stiffness of the antenna expressed in terms of minimum natural frequency of vibration above 1 Hz. Furthermore, various preliminary functional deployment tests of the antenna are performed and illustrated in this paper. In particular, the deployment accuracy tests need to meet the requirement of ±1 mm maximum difference between real deployed structure and its nominal dimensions. Finally, these deployment tests are used to validate the functionality of the deployment damper and the incorporated resettable mechanism. On one side the damper is necessary to control the velocity of the deployment and reduces the final mechanical shock at the end of the run and guarantees controlled deployment dynamics, whereas the resettable mechanism ensures an easy stowage process of the antenna for repeated deployments during qualification and acceptance ground testing campaigns.

1. INTRODUCTION

The electromagnetic performance of a helical antenna is determined by key geometrical parameters such as helix diameter, pitch or turn spacing, and the number of turns. These parameters influence whether the antenna operates in normal mode or axial mode. In normal mode, which occurs when the helix dimensions are much smaller than the wavelength, the antenna radiates a linearly polarized wave in a direction perpendicular to the helix axis [1]. However, this configuration produces low gain and is therefore generally unsuitable for satellite communication applications. On the other hand, axial mode is achieved when the circumference of the helix approaches one wavelength, typically between 0.75λ and 1.33λ, and the pitch angle is between 12° and 15°. In axial mode, the antenna radiates circularly polarized waves along its longitudinal axis, with gain increasing as a function of the number of turns and total helix length [2].

Three types of antenna shapes are commonly used: the helix, conical horn and the Conical Log Spiral (CLS). Most of these systems are passively deployed, which does not use any active components to deploy in orbit. Different performance characteristics can be achieved from the different shapes as well as varying the conductor pitch, diameter and height of the helix and number of turns [3]. For example, a hyper-compact collapsible antenna which can fit in a 0.5U CubeSat volume has been constructed using a framework of fiberglass and thermoplastic pultruded tape strips. For stowing, the structure needs to be rolled up into a self-deploying ball without creating plastic deformation or damaging the structure [4]. This compact and lightweight design has a deployed to stowed ratio of 300:1 with an overall assembly weight of 300 g. An origami folding technique has been implemented in another example of packable and tuneable multi-radii helical antenna [5]. This antenna has two separate foldable sections with the conductor wire wound around the perimeter. The structure is divided into two independent sections with different radii and the capability to adjust the height independently. In contrast, a conical-shaped spiral antenna is made from an Astro quartz-epoxy shell with the conductor element wrapped around the main cone structure in a logarithmically progressive manner [6]. To collapse the antenna, the cone structure has been divided into sections with hinges, such that it can be flattened and then folded for stowage. Concerning the helix type of antenna, other prototypes have the helicoid spiral acting as the main supporting structure and the conductor. This configuration has a stiff inner core with no electrical conductivity and a conductive coating applied on the surface with no mechanical stiffness [7]. Similarly, other prototypes use fabric membranes to increase the structural rigidity together with the main coil. In this case, the helicoid structure itself is manufactured to twice the extended length and compressed before slotting it into the fabric membrane, acting as a preloading mechanism increasing the stiffness of the antenna [8]. Similar passive helicoid antenna systems are already available in the market with possible customizations and operational range between 400 - 3000 MHz [9]. Other active antenna prototypes use stepper motors to control the deployment and adjust the final operating length of the helicoids [10]. Such systems ensure that the height and diameter are deployed correctly, however a more complex stowage technique is required. This deployment precision comes at the cost of a higher system mass, power consumption, mechanical complexity, and introduces various potential points of failure to consider in the antenna design.

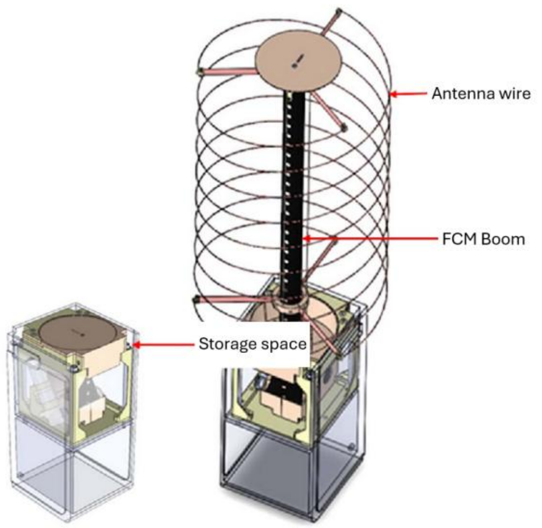

Figure 1 Deployable VHF/UHF helix antenna [10].

2. OBJECTIVES AND SCOPE

The purpose of this project is to develop an engineering model prototype of a passive deployable helicoid trifilar antenna. The design must comply with CubeSat dimensional constraints, with a height limit of the envelope of 20 mm. The antenna must be composed of three identical metal wires formed into helicoidal shapes and arranged at the base with a 120° phase offset. These three wires need to perform two functions: they act as the main deployable structure and as the electrical conductors.

The final antenna geometry must remain within the specified tolerances: the helicoid wire pitch, the final deployment height, outer diameter, concentricity and cylindricity of the perimetral antenna envelope must all remain within ±1 mm of their nominal values. In addition, the repeatability of the antenna deployment must be ensured, meaning that the specified tolerances are met in every deployment, regardless of how many times the antenna is stowed and deployed. Finally, the antenna deployment dynamics must be smooth and controlled, preventing any shock at the end of the travel.

The initial antenna design approach and electrical parameters are discussed in Section 3. The development of the first prototype is presented in Section 4, while Section 5 describes the helicoid forming process along with various bracing techniques supported by computational structural analysis. Finally, Section 6 reports the results of the deployment tests conducted to verify compliance with the requirements, including the accuracy and repeatability of the deployed antenna shape.

3. ELECTRICAL PERFORMANCE AND GEOMETRICAL DESIGN

The antenna's electrical performance, including gain and operating frequency band, dictates its geometrical configuration. Based on these requirements, parameters such as wire pitch, antenna height, and the outer diameter of the cylindrical envelope can be defined, within some range. The antenna is designed to operate in the UHF band between 0.86 GHz and 0.93 GHz, corresponding to IoT applications. In this design, the helix radius is set to 40 mm. With a pitch of nearly 70 mm a total length of 260 mm is reached in a few turns. These parameters are selected to approach axial-mode operation, ensuring suitable circular polarization and directive radiation characteristics.

The design of the deployable trifilar helix antenna is driven by the need to achieve circular polarization with stable radiation characteristics while remaining compatible with CubeSat volume constraints. In this configuration, three identical helicoidal conductors are symmetrically arranged around the antenna axis with an angular separation of 120°, forming a tri-helix structure. This geometry enables the generation of circular polarization through the proper excitation of the three arms, typically with equal amplitude and a progressive phase shift of 120°, thereby producing a rotating electromagnetic field along the antenna axis.

The feeding network represents another critical aspect of the trifilar configuration. To ensure proper circular polarization, the three helices must be excited with precise phase relationships. This can be achieved using a three-way power divider combined with phase-shifting elements or through an integrated feeding structure at the antenna base. The design must ensure equal amplitude distribution and minimal phase error, as any deviation can significantly degrade the axial ratio and introduce polarization ellipticity.

Finally, the interaction between the electrical and mechanical design must be carefully considered. Variations in the deployed geometry such as deviations in helix diameter, pitch, or alignment can lead to performance degradation, particularly in terms of gain and axial ratio. Therefore, strict manufacturing tolerances and highly repeatable deployment behaviour are essential to ensure consistent antenna performance across multiple deployment cycles.

At this stage, the work is divided into two main phases. On one hand, the manufacturing of the three antenna helicoids is addressed; on the other hand, various bracing techniques are investigated and implemented to deploy the antenna and maintain the three metal wires in position.

4. ANTENNA HELICOID MANUFACTURING

The helicoid formation process is crucial, as it determines the antenna's overall geometry. First, the helicoid forming process must be repeatable, since the three wires need to have identical shapes.

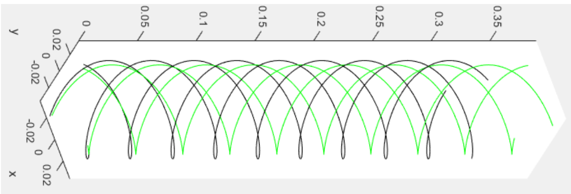

Figure 2 Free wire shape, no preload (green) and preloaded (black) wire shape of the antenna helicoids.

The implemented helicoid forming approach involves manufacturing a slightly longer helix with a smaller diameter, referred to as the construction / free wire shape helicoid (green in Figure 2). During the antenna assembly process, these helicoids are slightly compressed, allowing them to act as preloaded springs (black line in Figure 2). This ensures that the final antenna shape is achieved and maintained with a desired axial preloaded stiffness. Indeed, Figure 2 shows the theoretical free wire shape type of helicoids in green whereas the required antenna shape is illustrated with the black line.

Figure 3 Single helicoid compressed in stowed configuration.

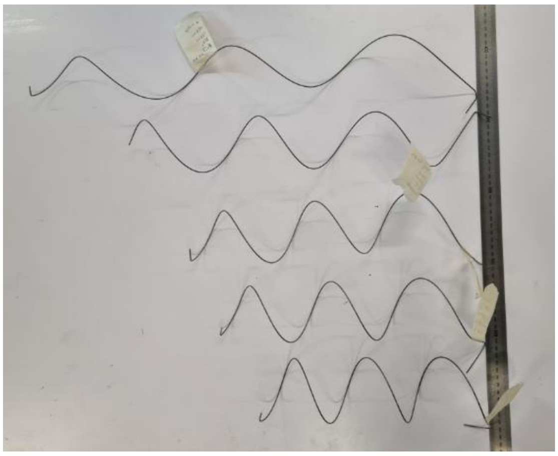

Figure 4 Various manufactured helicoidal wires.

A custom machine has been constructed in our laboratory, consisting of a rotating mandrel to which one end of the wire is firmly attached, while the other end is rigidly connected to a constant pulling force. With this setup, both the mandrel diameter and the angle of the pulling force can be finely adjusted within a specific range.

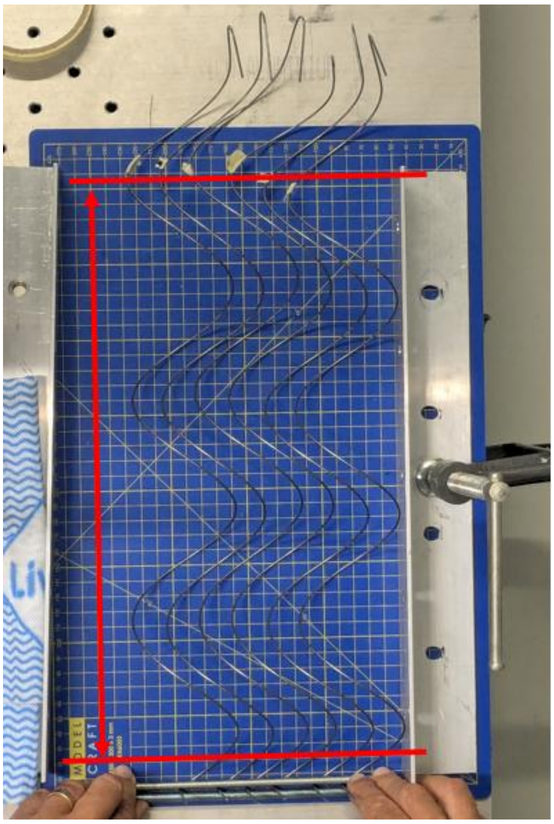

Figure 5 Antenna helicoids formation.

The mandrel diameter directly determines the antenna's outer diameter, whereas the pulling force angle mainly affects the wire pitch length and therefore the final length of the helicoid. Various diagrams were created experimentally to relate the mandrel diameter and the pulling force angle as a function of the selected steel wire diameter. As shown in Figure 4 several iterations of the helicoid forming process were necessary to achieve the desired final helix shape of the wire illustrated in Figure 5. The final goal is to create a metal conductive wire that can be stored at a minimum height, as shown in Figure 3, and then redeployed a certain number of times to the original helicoid shape as shown in Figure 5. The repeatability of the wire forming process is fundamental and crucial to ensure that all wires have the same curvature, helicoid pitch, and outer diameter.

5. ANTENNA STRUCTURE AND BRACING TECHNIQUE

To support the antenna structure, a telescopic beam concept inspired by compact umbrella mechanisms, in which nested segments would extend sequentially and lock in place via spring-loaded detents has been investigated, as illustrated in Figure 6A. This design was excluded for practical reasons, as integrating such detents within thin-walled telescopic components would have required precision machining and outsourced fabrication. Because physical prototyping plays a key role in the validation process, any design that cannot be implemented using accessible in-house manufacturing techniques, such as 3D printing, is considered incompatible with the objectives of maintaining low cost and simplicity.

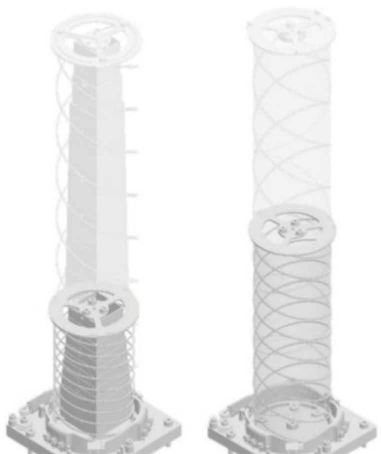

(a) (b)

Figure 6 Rendering of possible antenna internal supporting configurations. (a) telescopic beam concept (b) elastic mesh sleeve.

On the other hand, an elastic mesh sleeve made from space-grade film (Kapton or aluminised Mylar), designed to unwrap and assist deployment has also been considered as shown in Figure 6b. This design was ultimately discarded because of its higher material cost, the risk of electromagnetic interference, and the limited controllability of its strain-based actuation mechanism. The approach did not provide any clear benefit over the antenna's intrinsic elasticity and instead introduced additional assembly complexity.

5.1. INITIAL BRACING STRATEGY

Several alternative concepts for retaining the antenna structure were evaluated, including bistable rotary joints, bistable tape-spring joints, elastic detents, and tension springs. Nevertheless, the very limited packaging volume, the requirement for passive deployment, and affordability constraints prevented the use of more complex mechanisms. Therefore, approaches relying on additional components were discarded, and it was decided to control the deployment through mechanical damping and structural bracing.

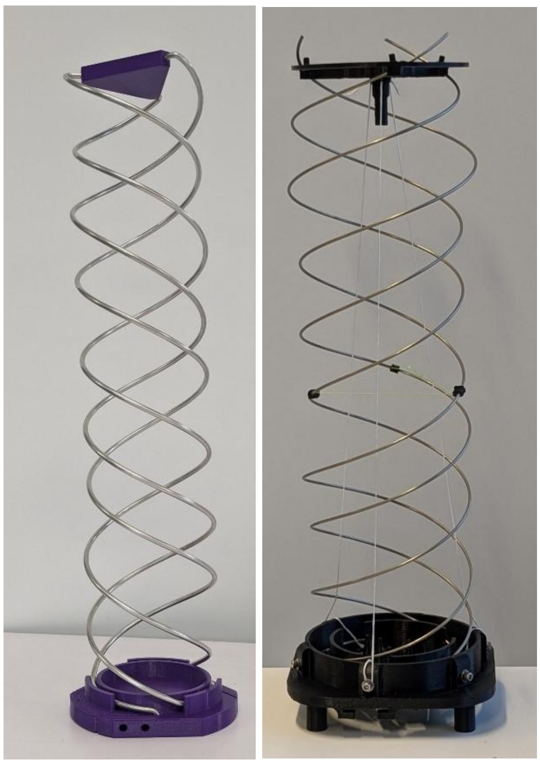

(a) (b)

Figure 7 Antenna prototypes: (a) Aluminium wire. (b) Steel wire.

The first prototype developed is illustrated in Figure 7a, where the helicoid shape is formed using an aluminium wire. This model is used to identify where potential critical features may occur; however, it has an inherent limitation. This aluminium wire antenna prototype cannot be stowed and compressed towards the base, as the aluminium yields and does not spring back to its initial deployed position. The second prototype is illustrated in Figure 7b, where a slightly thinner steel wire is employed. In this case, the elasticity of the three metal wires is sufficient to ensure the complete deployment of the antenna after being stowed at the

base as shown in Figure 3.
As described in Section 4, the helicoid wires were formed with an intentionally longer pitch length to axially preload the antenna to increase deployed stiffness.

To control and constrain the height of the antenna, three Dyneema wires are added in a pyramidal configuration and attached to the central point of the top junction element as shown in Figure 7 Antenna prototypes: (a) Aluminium wire. (b) Steel wire.b. In addition, the central points of the three helicoids at mid-height are mutually constrained by a second Dyneema wire feature arranged in a triangular configuration. This bracing solution effectively locks the central distance between the helicoids and the antenna height. However, the top interconnection element tends to slightly tilt, whereas the central part of the antenna helicoids tends to buckle toward one side and develop the common S-shaped curvature making this bracing solution unsuitable.

5.2. INTERNAL PYRAMIDAL BRACING

The second bracing technique investigated is shown in Figure 8. With this configuration, the antenna height is divided into three sections, each of which includes a flexible triangular connecting element designed to maintain the nominal spacing between the helicoids. In addition, three groups of concentric pyramidal wires are arranged from each of the three central points and tighten at the base as shown in Figure 8b. This bracing configuration ensures that the central point of the three antenna sections remains at the correct height, centred and aligned with the vertical axis also ensuring the concentricity of the three helicoids.

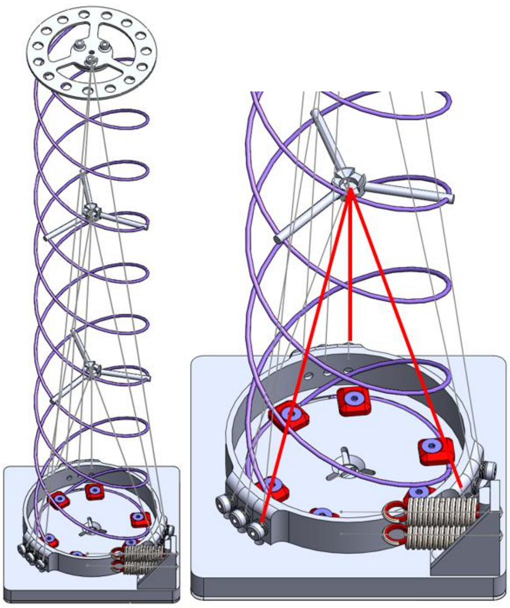

(a) (b)

Figure 8 Internal pyramid bracing technique.

However, first- and second-order buckling modes of the antenna, resulting in "C" or "S" shaped deformations, cannot be entirely avoided. This wire-lashing [MH1]technique uses nine wire strands arranged in three groups of different lengths that must be securely accommodated at the base during the antenna stowage process. This makes the procedure challenging and significantly increases the risk of the wires becoming tangled during deployment. In addition, due to the triangular pyramid configuration shown in Figure 8b, the Dyneema lines must pass from the inner side of the antenna to the outer side in order to be anchored to the base with the widest possible footprint.

5.3. OUTER PYRAMIDAL BRACING

The third bracing approach considered in this study is the external pyramid bracing technique. As illustrated in Figure 9, the antenna is divided into three sections, each of which uses three pairs of wire strands arranged in a triangular configuration and attached from the three central stellar arms to the antenna base. A detailed bracing scheme is shown in Figure 9b. With this configuration, the total number of wire strands increases to eighteen, which significantly raises the risk of tangling during deployment. However, the antenna buckling previously occurring is no longer an issue, since the tilt of the central sections can be minimized by precisely adjusting the antenna sections height using the three arms of each section's stellar element as control points for height and concentricity.

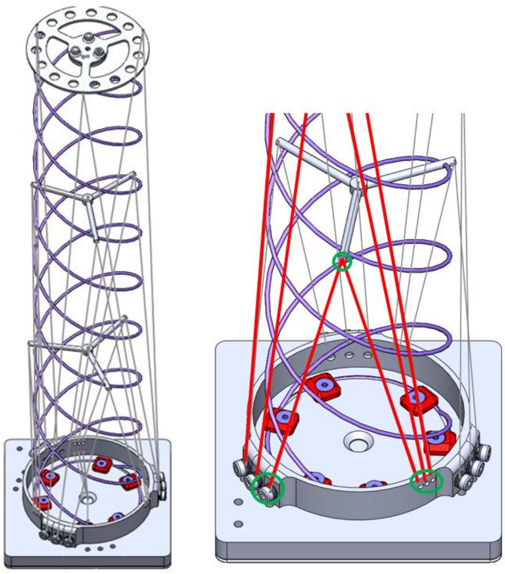

(a) (b)

Figure 9 External pyramid bracing technique.

Figure 10 Antenna prototype of the external pyramid bracing technique.

Each of these bracing techniques presents various advantages and disadvantages. A common issue, however, is that the large number of long wires running along the radiating elements poses a significant challenge during the stowing process, as it requires meticulous arrangement at the antenna base. A major problem also arises during deployment, since the wires can repeatedly become entangled with each other and with other antenna components, such as the stellar spacer arms located at mid height and the base itself.

5.4. PREFERED BRACING TECHNIQUE

For these reasons, a completely different type of bracing arrangement is required, and therefore a triangular wiring network applied along the antenna structure is investigated. As shown in Figure 11, the triangular net configuration connects two consecutive metal wires at three points, a, b, and c, forming the corresponding angles α, β and γ. To determine the optimal arrangement of the Dyneema bracing wires, a finite element (FE) analysis simulation is implemented in Ansys APDL.

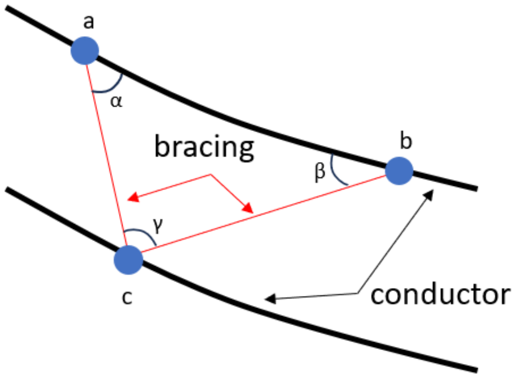

Figure 11 Triangular bracing net technique.

The simulation begins by importing the slightly longer formed helicoid wires, as manufactured from the description in Section 4. Various anchor points are then identified along the metal helicoid wires to create a triangular mesh as depicted with the blue points in Figure 11. A specific rigid displacement is then applied at each blue anchor point. This rigid displacement moves each blue anchor point of the three helicoids from the free / non-compressed configuration toward their final positions, creating the preloaded configuration by slightly compressing the helicoids. At this stage, a stress field is generated in the metal wires and consequently the direction of the resultant of the reaction forces acting on each of the preselected blue anchoring points indicates the orientation along which the Dyneema wire should be placed to brace the antenna.

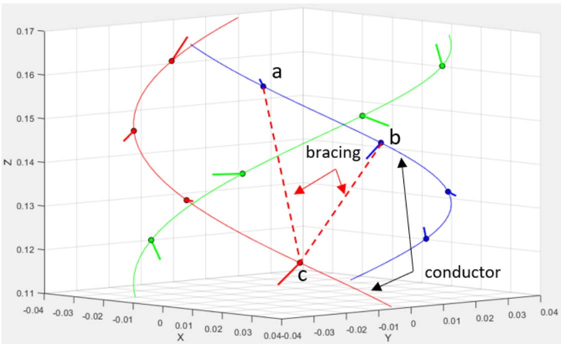

Figure 12 Antenna bracing pattern.

The three metal helicoid wires are schematically shown in red, blue and green in Figure 12. As a result of the simulation, the reaction forces that are acting on each anchoring point are illustrated with the respective colour. Therefore, the selected triangular bracing scheme is depicted with the dashed red line connecting the points a, b, and c.

The antenna bracing, in addition to ensuring the correct alignment between the wires, must also provide sufficient axial stiffness together with the applied preload in order to guarantee the minimum natural frequency of lateral oscillation in the deployed configuration. This requirement is very important to ensure that any oscillations of the deployed antenna do not interfere with the satellite attitude control system (ACS) during an orbital manoeuvre. In general, a safe requirement requires the natural frequency of a satellite appendage [MH2]to be higher than 1 Hz, but this requirement can vary from application to application. Consequently, a pre-stressed modal analysis is performed to investigate the natural modes of the braced structure.

5.5. PRE-STRESSED MODAL ANALYSIS

The final braced and axially preloaded configuration of the antenna structure, as investigated in Section 5.4, is imported to perform the prestressed modal analysis. The wire bracing pattern shown in Figure 11 is applied to the three helicoidal metal wires using spring elements connected to the group of specific selected nodes (anchor blue points in Figure 11).

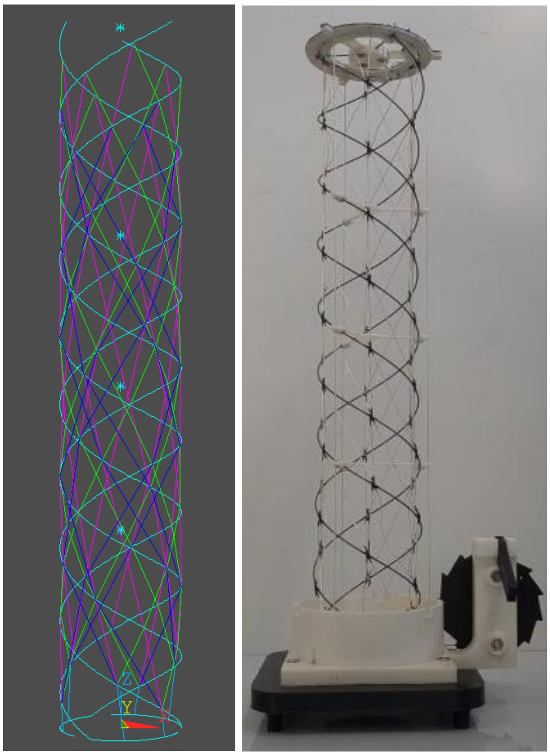

(a) (b)

Figure 13 Antena bracing structure. (a) finite element antenna model (b) Physical antenna prototype.

Furthermore, four concentrated mass elements are introduced along the vertical central axis to represent the star-shaped spacing components.

The static structural analysis previously performed to establish the antenna axial preload (see Section 5.4) is now restarted. This additional step accounts for element stress redistribution and structural relaxation, as the preloaded antenna configuration is now held in place by the triangular bracing wire net.

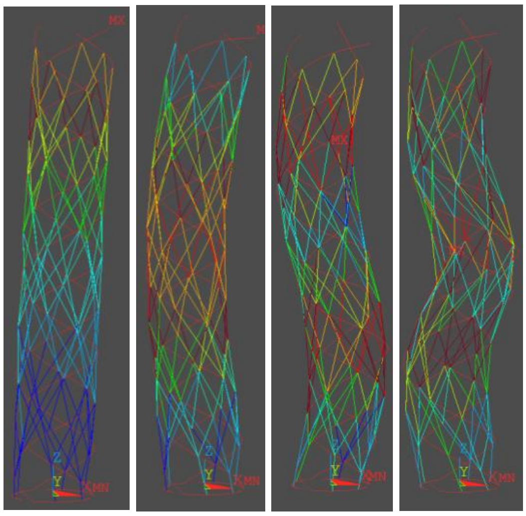

(a) (b) (c) (d)

Figure 14 Antenna natural modes.

Finally, the prestress modal analysis is performed. The first set of the eigenmodes of the antenna are illustrated in Figure 14, while the respective eigenfrequencies are reported in Table 1.

Table 1 Antenna natural frequencies.

Natural mode	Frequency [Hz]
1st and 2nd	5.8
3rd and 4th	28
5th and 6th	38
7th and 8th	66

6. DYNAMIC DEPLOYMENT TESTS

After several design iterations and structural simulations, the antenna is ultimately manufactured using the bracing pattern developed in Sections 5.4 and 5.5. Moreover, the 3D-printed antenna base is designed and manufactured to support the lower interface of the helicoid wires and provide a structural frame for stowage. The base needs to be compatible with standard CubeSat integration requirements, featuring a footprint of 100 × 100 mm.

A central cylindrical cavity is incorporated to accommodate the three helicoid wires in their compressed configuration, along with the bracing wires, which are carefully folded toward the centre. Furthermore, the upper interconnection element of the helicoidal wires also includes dedicated indentations and locking features to ensure secure engagement with the antenna base when stowed.

a b c

Figure 15 Antenna dynamic deployment tests.

At this stage, a large number of deployment tests are conducted to evaluate the dynamic behaviour of the system, particularly in terms of deployment velocity and end-of-stroke shock. These tests are also essential to assess the repeatability of the antenna deployment, ensuring that the structure consistently reaches the same deployed height, by maintaining the concentricity and cylindricity of the helicoid's perimeter within the specified geometric requirements with a tolerance of ±1 mm.

The implemented procedure consists of repeatedly stowing and deploying the antenna, capturing images from a fixed distance, and comparing them to evaluate deployment repeatability. As illustrated in Figure 15, three examples of deployment tests are presented together with the measurement experimental setup which includes a set of graduated scale markings mounted on a white background to measure the antenna height. In addition, a digital height gauge is positioned laterally. Therefore, after each deployment test, the antenna height is accurately measured, and the structure is rotated through a full revolution about a fixed pivot point at the base to assess the concentricity at the top. The results are very encouraging: the antenna height consistently remains within the ±1 mm tolerance, while the radial variation of the top concentricity remains within ±2 mm.

7. CONCLUSIONS

This work aims to present the initial design and prototyping steps of the engineering model of a trifilar helicoid antenna. The requirements include the development of a single metal structure capable of acting both as the primary supporting structure and as the radiating elements of the antenna. In addition, the model must be cost-effective to manufacture, easy to assemble, and capable of ensuring repeatable deployments while maintaining the final deployed geometry within a tolerance of ±1 mm.

Following several design and simulation iterations, the antenna is manufactured, and a series of deployment tests are conducted to verify compliance with the project requirements. The deployment height accuracy is successfully achieved; however, the concentricity shows a slight deviation beyond the desired tolerance. Furthermore, it is observed that the end-of-stroke shock is significant in this configuration, as the energy stored in the compressed wires is relatively high. For this reason, the integration of a damper is recommended to better control the deployment dynamics.

8. REFERENCES

1. C. A. Balanis, *Antenna Theory: Analysis and Design*. New York, NY, USA: Wiley, 1982.
2. G. Slade, *The Basics of Quadrifilar Helix Antennas*. Highfields, QLD, Australia: QSL.net Publishing, 2015.
3. J. Costantine, S. Pellegrino, and M. Sakovsky, "Rapid design of deployable antennas for CubeSats: A tool to help designers compare and select antenna topologies," in *Proc. 31st Annual AIAA/USU Conf. Small Satellites*, Logan, UT, USA, Aug. 2017.
4. D. J. Ochoa, K. Hummer, and M. Ciffone, "Deployable helical antenna for nano-satellites," in *Proceedings of the 28th Annual AIAA/USU Conference on Small Satellites*, Logan, UT, USA, Aug. 2014, pp. 1–7
5. C. L. Zekios, S. V. Georgakopoulos, and X. Liu, "Analysis of a packable and tunable origami multi-radii helical antenna," in *Proc. IEEE Int. Symp. Antennas and Propagation and USNC-URSI Radio Science Meeting*, Atlanta, GA, USA, Jul. 2019.
6. G. Christodoulou, J. Costantine, G. Olson, I. Maqueda, S. Pellegrino, M. Sakovsky, and Y. Tawk, "UHF deployable helical antennas for CubeSats," in *Proc. IEEE Antennas and Propagation Society Int. Symp. (APSURSI)*, Memphis, TN, USA, Jul. 2014.
7. J. Block, A. Bäger, T. D. J. Behrens, L.-C. Hauer, M. Schütze, R. Schütze, and T. Spröwitz, "A self-deploying and self-stabilizing helical antenna for small satellites," in *Proc. 7th Eur. Conf. Antennas Propag. (EuCAP)*, Gothenburg, Sweden, Apr. 2013.
8. M. Sureda, M. Sobrino, O. Millán, A. Aguilella, A. Solanellas, M. Badia, J. F. Muñoz-Martín, L. Fernández, J. A. Ruiz-De-Azua, and A. Camps, "Design and testing of a helix antenna deployment system for a 1U CubeSat," *IEEE Access*, vol. 9, pp. 66103–66114, 2021, doi: 10.1109/ACCESS.2021.3075660.
9. Helical Communication Technologies (HCT), "Helios deployable antenna," 2016.

https://www.cubesatshop.com/product/helios-deployable-antenna/

10. T. Huang, J. R. Reveles, Q. Harrington, V. Fraux, and V. Vinoth Gurusamy, "An innovative deployable VHF/UHF helical antenna for nanosatellites," in *Proc. 13th Eur. Conf. Antennas Propag. (EuCAP)*, Krakow, Poland, Mar.–Apr. 2019.